Resonant Jets for Turbine Cooling.

WASHINGTON UNIV SEATTLE

25 APR 1991

UNCLASSIFIED
SECURITY CLASSIFICATION OF THIS PAGE

REPORT DOCUMENTATION PAGE

1a. REPORT SECURITY CLASSIFICATION: UNCLASSIFIED	1b. RESTRICTIVE MARKINGS
2a. SECURITY CLASSIFICATION AUTHORITY	3. DISTRIBUTION/AVAILABILITY OF REPORT: Approved for public release, distribution unlimited
2b. DECLASSIFICATION/DOWNGRADING SCHEDULE: UNCLASSIFIED	
4. PERFORMING ORGANIZATION REPORT NUMBER(S)	5. MONITORING ORGANIZATION REPORT NUMBER(S)
6a. NAME OF PERFORMING ORGANIZATION: University of Washington; 6b. OFFICE SYMBOL (If applicable)	7a. NAME OF MONITORING ORGANIZATION: AFOSR/NA Bolling AFB DC 20332-6448
6c. ADDRESS (City, State, and ZIP Code): Seattle, WA 98195	7b. ADDRESS (City, State, and ZIP Code): AFOSR/NA Bolling AFB DC 20332-6448
8a. NAME OF FUNDING/SPONSORING ORGANIZATION: Air Force Office of Scientific Research; 8b. OFFICE SYMBOL (If applicable): NA	9. PROCUREMENT INSTRUMENT IDENTIFICATION NUMBER: F49620-88-C-0041
8c. ADDRESS (City, State, and ZIP Code): Building 41, Boiling Air Force Base, D.C. 20332-6448	10. SOURCE OF FUNDING NUMBERS: PROGRAM ELEMENT NO. 61102F; PROJECT 2307; TASK NO. A/4; WORK UNIT ACCESSION NO.

11. TITLE (Include Security Classification)
Resonant Jets for Turbine Cooling (Unclassified)

12. PERSONAL AUTHOR(S)
M. Kurosaka

13a. TYPE OF REPORT	13b. TIME COVERED	14. DATE OF REPORT (Year, Month, Day)	15. PAGE COUNT
Final Report	FROM 1/1989 TO 2/91	1991, April 25	22

16. SUPPLEMENTARY NOTATION

17. COSATI CODES			18. SUBJECT TERMS (Continue on reverse if necessary and identify by block number)
FIELD	GROUP	SUB-GROUP	

19. ABSTRACT (Continue on reverse if necessary and identify by block number)
The objective of the present investigation is to enhance the effectiveness of jet-impingement cooling, used in the hot turbine sections of aircraft engines, by exploiting the recently recognized capacity of the large-scale structures to alter the total temperature of jets. In this report, the results obtained from (1) a newly constructed air-jet facility and from (2) a water-jet test rig built separately for flow-visualization study are described. In each, a jet discharged from a circular nozzle impinges on a plate. The results appear to substantiate the following speculations previously advanced: The secondary vortices, which are induced by the bombardment of the primary vortices formed initially at the nozzle exhaust, are responsible for the cooling on the impingement surface. The degree of cooling is, however, significantly affected by the competition between the primary and secondary vortices and the occurrence of acoustic resonance. The effect of the curvature of the impingement plate and the jet Mach number is also described.

20. DISTRIBUTION/AVAILABILITY OF ABSTRACT	21. ABSTRACT SECURITY CLASSIFICATION
☒ UNCLASSIFIED/UNLIMITED ☐ SAME AS RPT. ☐ DTIC USERS	UNCLASSIFIED
22a. NAME OF RESPONSIBLE INDIVIDUAL: MAJOR D. FANT	22b. TELEPHONE (Include Area Code): 202-767-0471; 22c. OFFICE SYMBOL: NE OSR/NA

DD FORM 1473, 84 MAR — 83 APR edition may be used until exhausted. All other editions are obsolete.

SECURITY CLASSIFICATION OF THIS PAGE

UNCLASSIFIED

(1) ***Title:*** Resonants Jets for Turbine Cooling

(2) ***Overall Objective:*** To enhance the cooling effectiveness of jet-impingement cooling, used in the hot turbine section of aircraft engines, by exploiting the recently recognized capacity of large-scale vortical structure to alter the total temperature of jets

(3) ***Contract Number:*** F49620-88-C-0041

(4) ***Principal Investigator:*** M. Kurosaka, Professor
Department of Aeronautics and Astronautics
University of Washington
Seattle, WA 98195

(5) ***Contract Period:*** January, 1988 to February, 1991

(6) ***Report Date:*** April, 1991

(7) ***Discussion on the Program:*** Objectives, background and present tasks

(7a) ***Air-Force Needs***

Compared to the present thrust-to-weight ratios of the current military aircraft engines, which is, for instance, about 6 for F101, the far-term target in the year 2000 and beyond is aimed at the values of 14-16, more than twice of those achieved in the technology of today. As a key component improvement to push toward such a goal, the turbine temperature is envisioned to be raised from the current level of 2400°F to 3600°F; therefore, the increase of the hot section cooling by the amount of 80% or more, without incurring weight penalty, is considered to be an imperative.

(7b) ***Background A - Impingement cooling in aircraft engines***

Among various schemes used to cool the turbine hot sections, impingement cooling is one of crucial importance inasmuch as it provides cooling to the leading edges of the turbine stators and rotors, the region exposed directly to the high-temperature air discharged from combustors.

In impingement cooling, a jet is directed towards the leading edge of the turbine vanes in order to avoid local hot spots. This is accomplished by inserting a tube inside the hollow airfoil and orienting the insert so that the series of holes, machined into the nose of the insert,are opposite to the inside surface of the leading edge. Cooling air extracted from the compressor is introduced into the insert and exits through the holes as a series of jets directed at the leading edge.

High levels of heat transfer are desirable in the midchord region, too and this is often accomplished by the impingement cooling. Impingement cooling is also utilized for the high-temperature combustion liners in order to provide thermal protection.

Present aircraft engines require a large amount of cooling flow, of the order of 20% of the compressor discharge: the cooling air bled from the compressor is not fully recoverable for turbine output. In order to minimize the quantity of the cooling air anticipated for future aircraft operating at higher temperatures, efforts are intensified in developing such advanced technologies as shower-head cooling for the leading edge and the shingle liner concept for combustors.

(7c) ***Background B - Large-scale vortical structures around the jet periphery***

Turning our attention to the flow structure of the jets in general, they can be viewed as mixing layers in circular form. Then, in light of the now well-established presence of coherent large-scale structures in a plane mixing layer--even at the condition where the flow had been traditionally considered to be disorderly and featureless, it is not surprising to find orderly structure even in the circular jets at high Reynolds numbers. Thus the structure of vortex rings, long familiar in lower Reynolds number flows, is observable even at higher Reynolds number flows, which are in the range corresponding to impingement cooling.

This large-scale structure is not limited to subsonic jet flows; even in supersonic jets, the instability waves are persistently present.

The vortex-ring structures can be acoustically intensified by the provision of a sound source tuned to the frequency of natural unstable disturbances.

(7d) ***Background C - Total temperature separation in the wakes***

To pave the way for the discussion of the total temperature separation in jets, here we present what is known in a similar large-scale structure in wake flows. It has recently been demonstrated, both experimentally and theoretically (Ref. 1), that the vortex street found behind a body has the capacity to separate the total temperature (T_t) around vortices, even when T_t is initially uniform. The basic process for this is *inviscid*; the total temperature separation is governed by the inviscid unsteady energy equation

$$c_p \frac{DT_t}{Dt} = \frac{1}{\rho} \frac{\partial p}{\partial t} .$$

The separation mechanism comprises these key ingredients: (i) the low-pressure fields at the vortex centers, (ii) their convective movement and (iii) the entrainment of fluid particles into the wake and their ejection out of it.

The unsteady separation of T_t around vortices thus predicted is indeed substantiated by the direct measurement obtained by an aspirating probe (Ref. 2).

Once time-averaged, the mean flow field conceals the presence of hot spots in the instantaneous flow. The time-averaged flow takes the guise of colder wake, with lowered T_t ; similarly the time-averaged total pressure in the wake shows only the defect.

(7e) ***Description of present program***

Using the facts described above as the building blocks, we aim to enhance the effectiveness of impingement cooling by exploiting the capacity of jet vortices to lower its total temperature. The major tasks are two fold.

TASK 1. Total temperature separation in a free jet

For simplicity, we consider first a free jet without an impinging wall. When we link the mechanism of the total temperature separation in the vortex street with the presence of the vortex rings even at high Reynolds number flows, it is immediately expected that T_t become separated around vortex rings in jets. Due to the rotational direction of the vortex rings in jets, which is opposite to that of the vortex street in the wake, the positions of hot and cold spots relative to the vortices are reversed from those in the wake: in an instantaneous snapshot, hot spots are expected to be located on the side of the jet centerline and cold spots on the freestream side (see figure 1).

The T_t separation should occur even in a situation where the initial temperature of the jet at the nozzle exit is selected to be the same as that of the surrounding air.

Even after being time-averaged, a free jet should retain the imprint of the instantaneous T_t separation. Substantiation of these points is one of the objectives of this investigation.

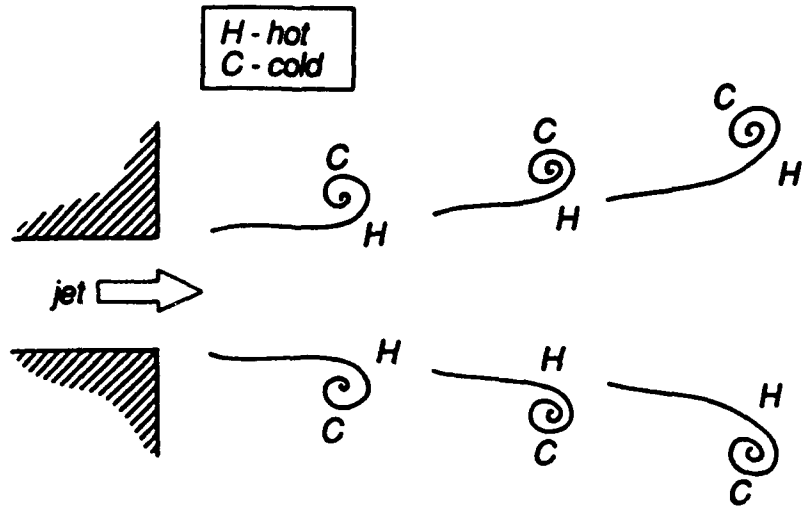

Figure 1. T_t separation in a free jet.

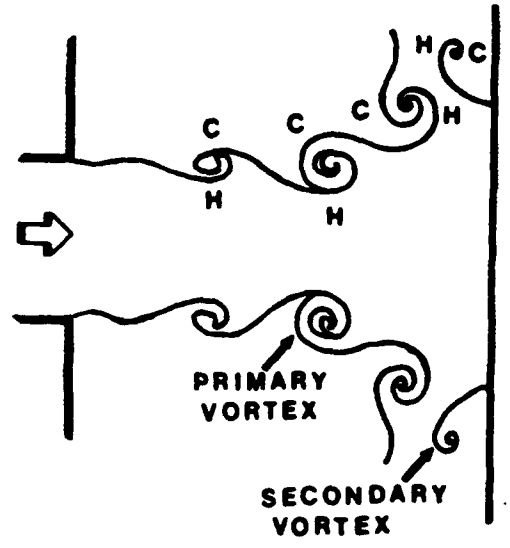

Figure 2. T_t separation in an impinging jet.

TASK 2. Total temperature separation in impinging jet

When an impingement plate is inserted in a jet, the T_t separation in the resulting impinging jet is modified by two processes: (1) additional vortices (secondary) induced by the approach of the aforementioned vortices (primary), and (2) acoustic resonance. Both will be explained in some detail below.

As is well known, the approach of a vortex causes an unsteady adverse pressure gradient on an impingement surface. Thus the approaching primary vortex ring induces the separation of the boundary layer on the surface into a counter-rotating secondary vortex ring. The competing influence of these two vortex rings results in the presence of hot and cold spots on the impingement surface, as shown in figure 2. Consider the case when the ratio of nozzle impingement plate spacing (x) to nozzle diameter (d) is small. The primary vortices will approach the surface near the stagnation point, where the momentum of the wall boundary layer is low. The unsteady adverse pressure gradients will overwhelm the low momentum, and cause the boundary layer to separate and roll up into secondary vortices. Since the secondary vortices are generated near the stagnation point and the rotation of the secondary vortices is opposite to that of the primary vortices, this will result in only a region of cooling on the impingement surface. At large x/d , however, the primary vortices approach the plate at a larger radial distance from the stagnation point. The boundary layer momentum is greater, and no separation occurs. With the absence of secondary vortices, the primary vortices result in heating on the plate surface.

Acoustic resonance strengthens the vortical structures in an impinging jet, thereby increasing the magnitude of the T_t separation on the impingement surface. The mechanism can be described as follows: when the primary vortex ring with its lowered pressure at the center is generated at time $t = 0$ (top of fig. 3) and impinges on the wall, a low-pressure acoustic wave is emitted (middle). If this low-pressure wave reaches the nozzle lip just at the moment a new vortex ring is forming (bottom), the vortex ring is intensified. When this new vortex ring impacts on the wall, a correspondingly stronger acoustic wave is emitted, and resonance develops. The condition for this "convective" resonance can be expressed in the form

$$\frac{x}{u_v} + \frac{x}{a} = \frac{n}{f_v}; \quad n = 1, 2, 3 \ldots \tag{1}$$

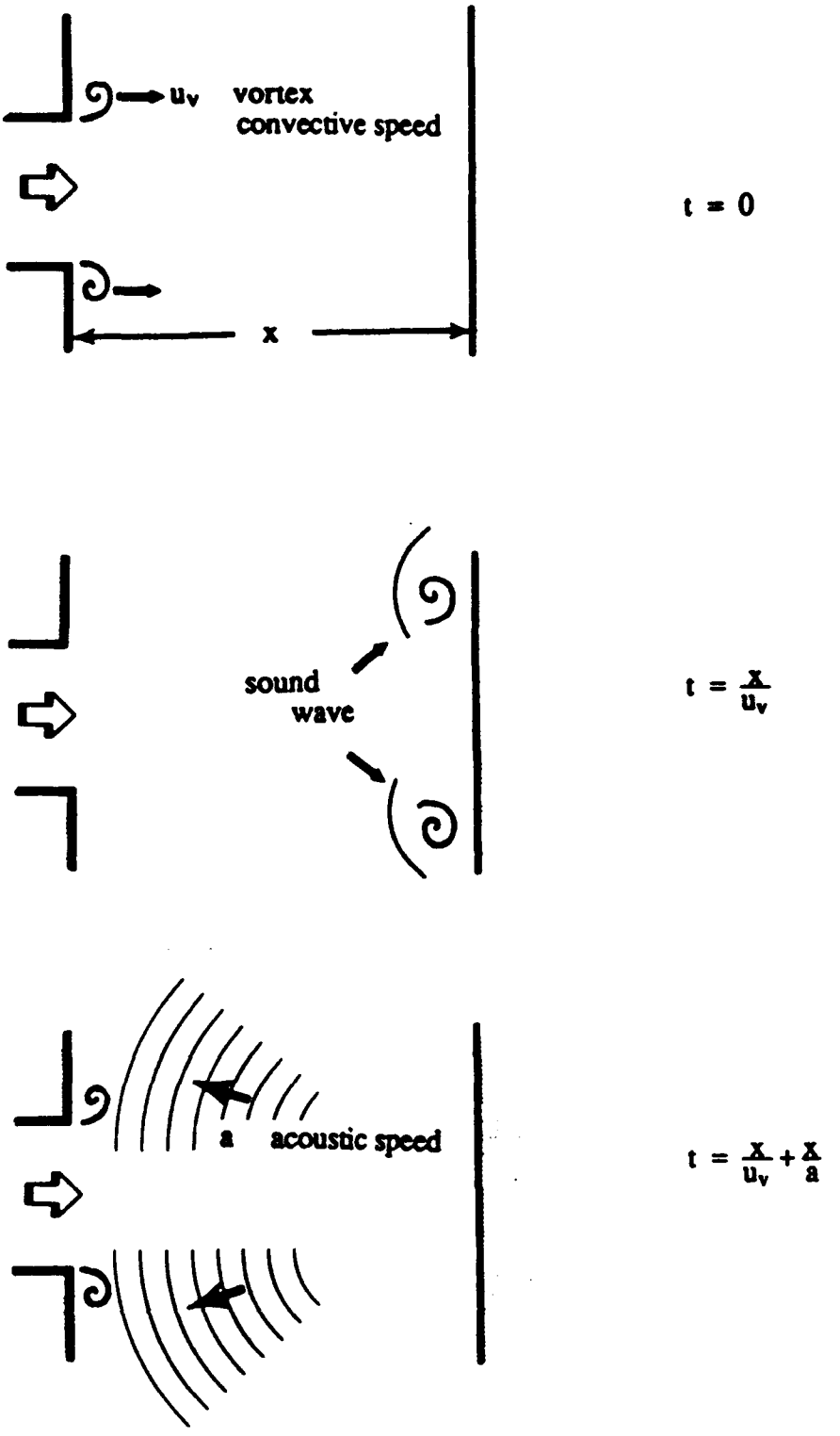

Figure 3. Mechanism of acoustic resonance.

where u_v is the convective velocity of the vortex rings, a is the acoustic speed, and f_v is the vortex shedding frequency.

In addition, an acoustic wave, standing between the wall adjacent to the nozzle and the impingement plate, can be produced in the otherwise quiescent air outside of the jet. Its frequency is given by

$$f_s = \frac{an}{2x}; \quad n = 1, 2, 3 \ldots \tag{2}$$

The level of resonance and thus T_t separation is expected to be greatest when the convective resonance of equation (1) occurs and, simultaneously, the standing acoustic wave frequency of equation (2) also matches the vortex shedding frequency (f_v).

The main objectives of Task 2 are to confirm (1) the competing effect of the primary and secondary vortices in inducing hot and cold spots and (2) their intensification by acoustic resonance.

(8) ***Results***

Two experimental facilities, the air-jet and water-jet facility, were constructed for this investigation. In the air-jet facility (figure 4) air supplied in blow-down fashion is heated to adjust the incoming air T_t and maintain it constant during a test. Jet background noise is reduced by a foam-lined flow-straightener section, and the nozzle (interchangeable from 1/8" to 4" diameter) and impingement plate are located in a test chamber designed to eliminate spurious sound. The sound level in the test chamber is measured by a condenser microphone. The impingement plate surface is instrumented with 88 thermocouples and 46 pressure taps, and the distance between plate and nozzle is controlled to an accuracy of 0.001" by a digital stepping motor. Tests were conducted with jet Mach number (M_j) ranging from subsonic to supersonic and with x/d ranging from 0.25 to 30.

The test section of the air facility is made in such a way to be convertible for the investigation of the synthetic secondary vortices to be described later.

The water-jet facility (figure 5) was constructed in order to conduct a flow-visualization study. Both the nozzle and the impingement plate are fitted with dye taps to allow visualization of the primary or secondary vortices alone, or together.

The results obtained from these facilities will be presented next.

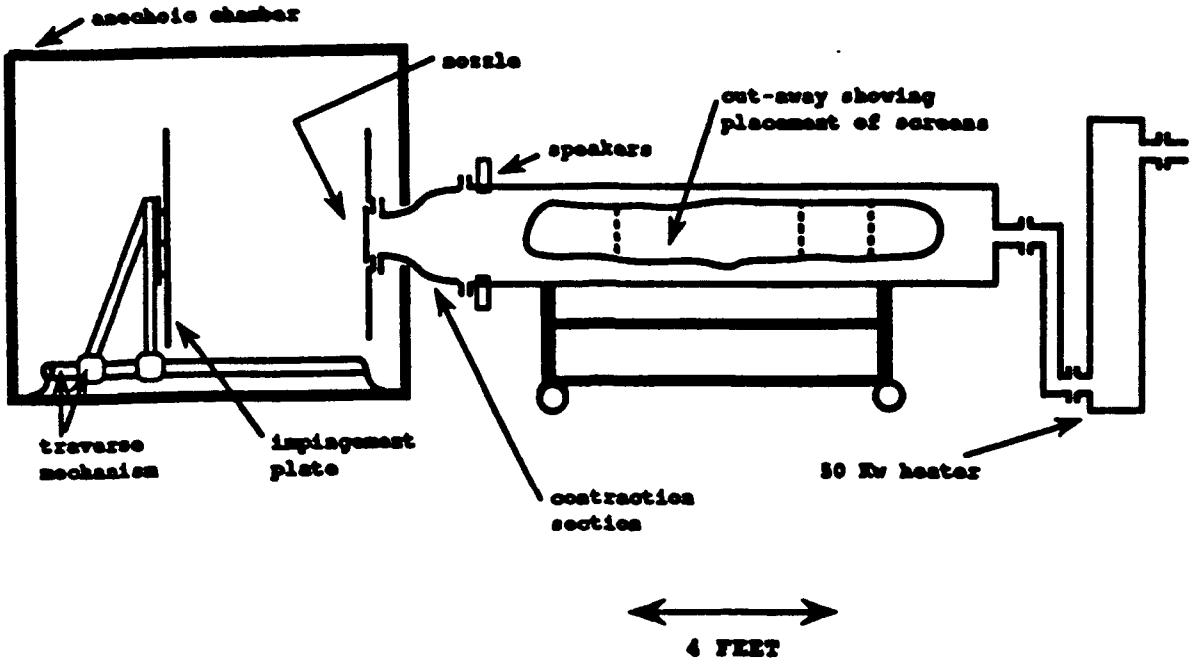

Figure 4. Air-jet facility.

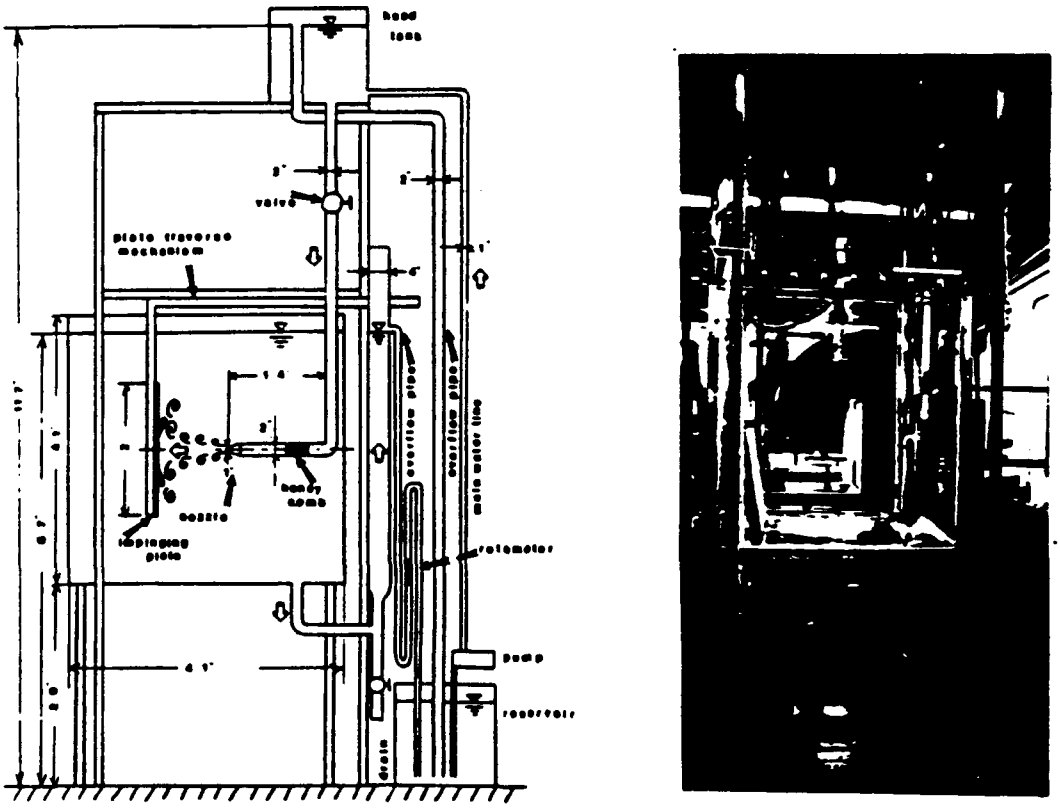

Figure 5. Water jet facility.

8.1 *Free Jet Results*

The time-averaged T_t distribution in a free jet is plotted in figure 6, for several values of x/d. For these tests $M_j = 0.9$ and the reservoir T_t is held constant and equal to the ambient T_t. Shown on the left side of the figure, for comparison, is the uniform T_t distribution that would occur in the absence of large-scale vortical structures. The measured T_t agrees quite favorably with the physical expectations discussed earlier. The near-field is characterized by a sharp T_t separation, and this becomes spread out as x/d increases. In the far-field the cooling has not completely disappeared, although it is greatly reduced in magnitude.

In order to confirm that the T_t separation increases as the strength of the vortex rings is intensified, the vortices are excited acoustically by four speakers mounted on the settling tank. The speaker frequency is tuned to 1137 Hz, the shedding frequency of the vortex rings corresponding to $M_j = 007$ and $d = 4"$. The results, shown in figure 7, clearly demonstrates that the T_t separation becomes enhanced in tone-excited jets.

8.2 *Impinging Jet Results*

8.2(a) *Flow Visualization Study and Baseline Data*

Flow visualization results obtained in the water jet facility support the vortex model suggested earlier. Primary vortices, formed at the nozzle lip, approach the impingement surface and generate counter-rotating secondary vortices, which then move in phase with the primary vortices. In other words, each of the secondary vortices formed in a row is precisely locked to, and moves with the corresponding primary vortex. Plate 1 contains a series of photographs showing both the secondary and primary vortices alone, and together. Furthermore, it is observed that the secondary vortices are present only when $x/d < 6$, in agreement with the theoretical expectation stated in (7e).

Typical radial distributions of the time-averaged wall temperature (T_w) and wall pressure (p_w) are shown side by side in figure 8. A notable feature is the presence of suction on the impingement surface at small values of x/d. The radial position of the suction roughly corresponds to that of the minimum T_w, and represents a "footprint" of the low-pressure cores of the secondary vortices. As seen from the flow visualization photos, the secondary vortices persist for a large radial distance, and form

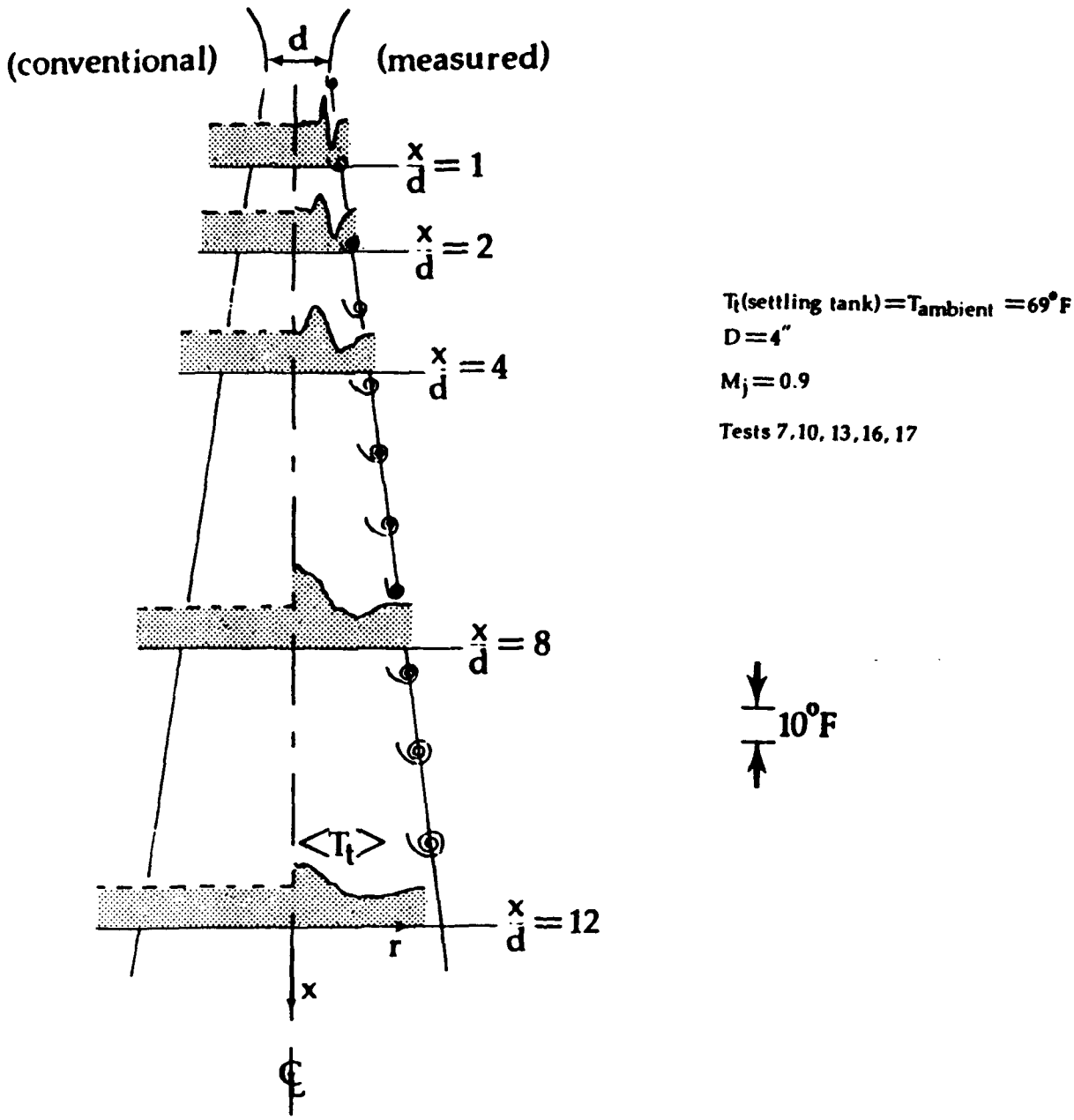

Figure 6. Radial distribution of time-averaged T_t in a free jet.

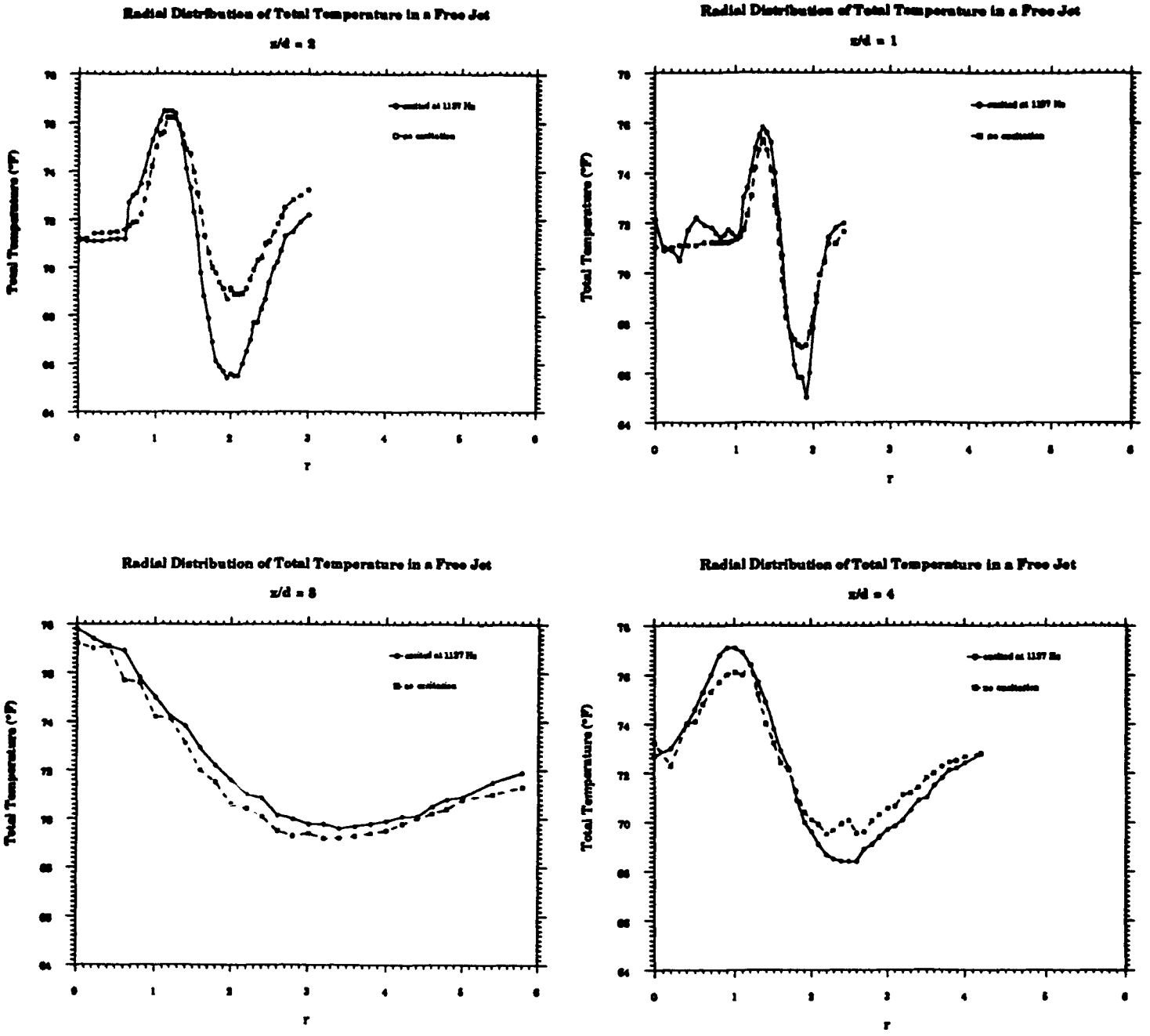

Figure 7. Effect of acoustic excitation on time-averaged T_t in a free jet.

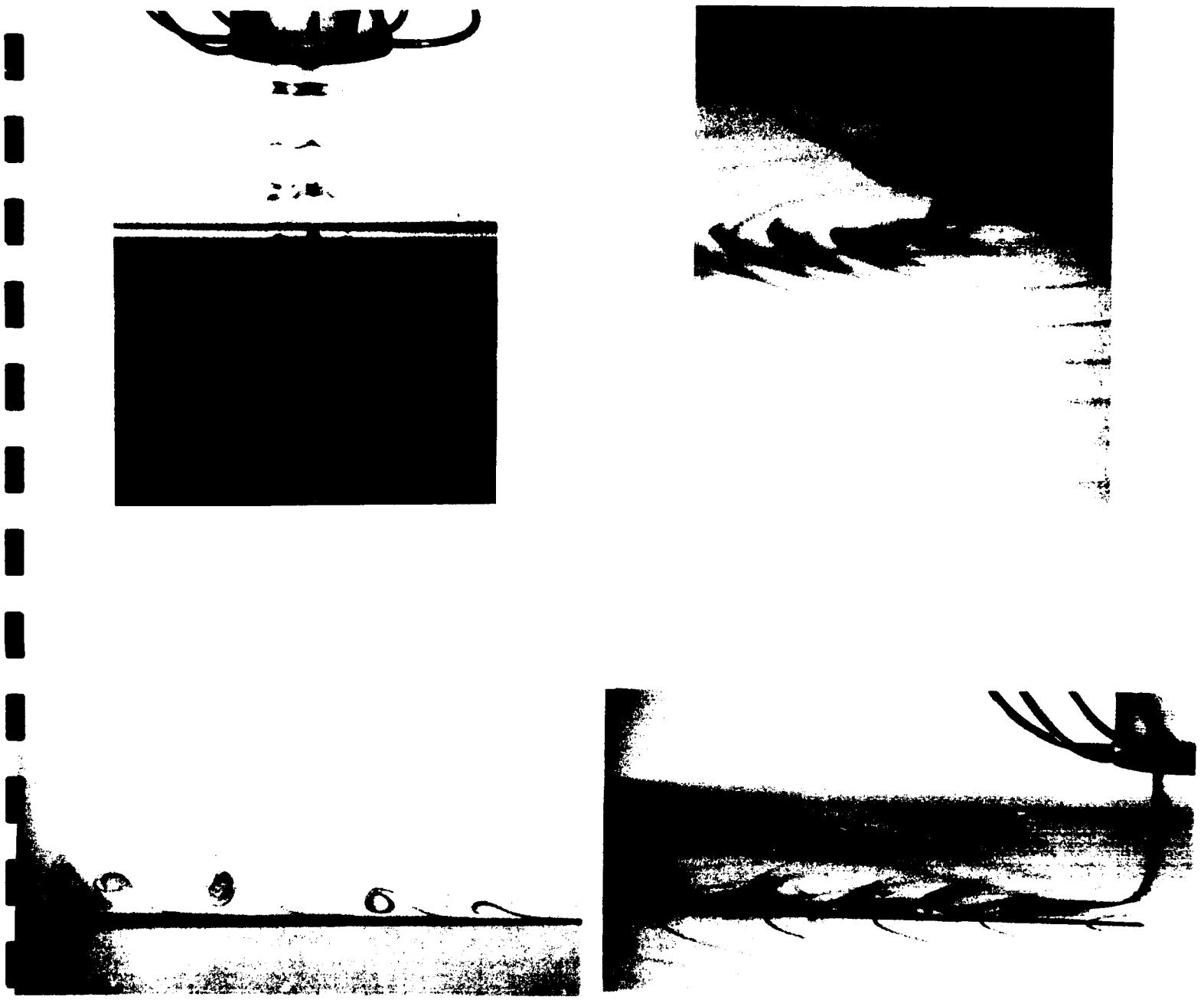

Plate 1. Flow visualization results.

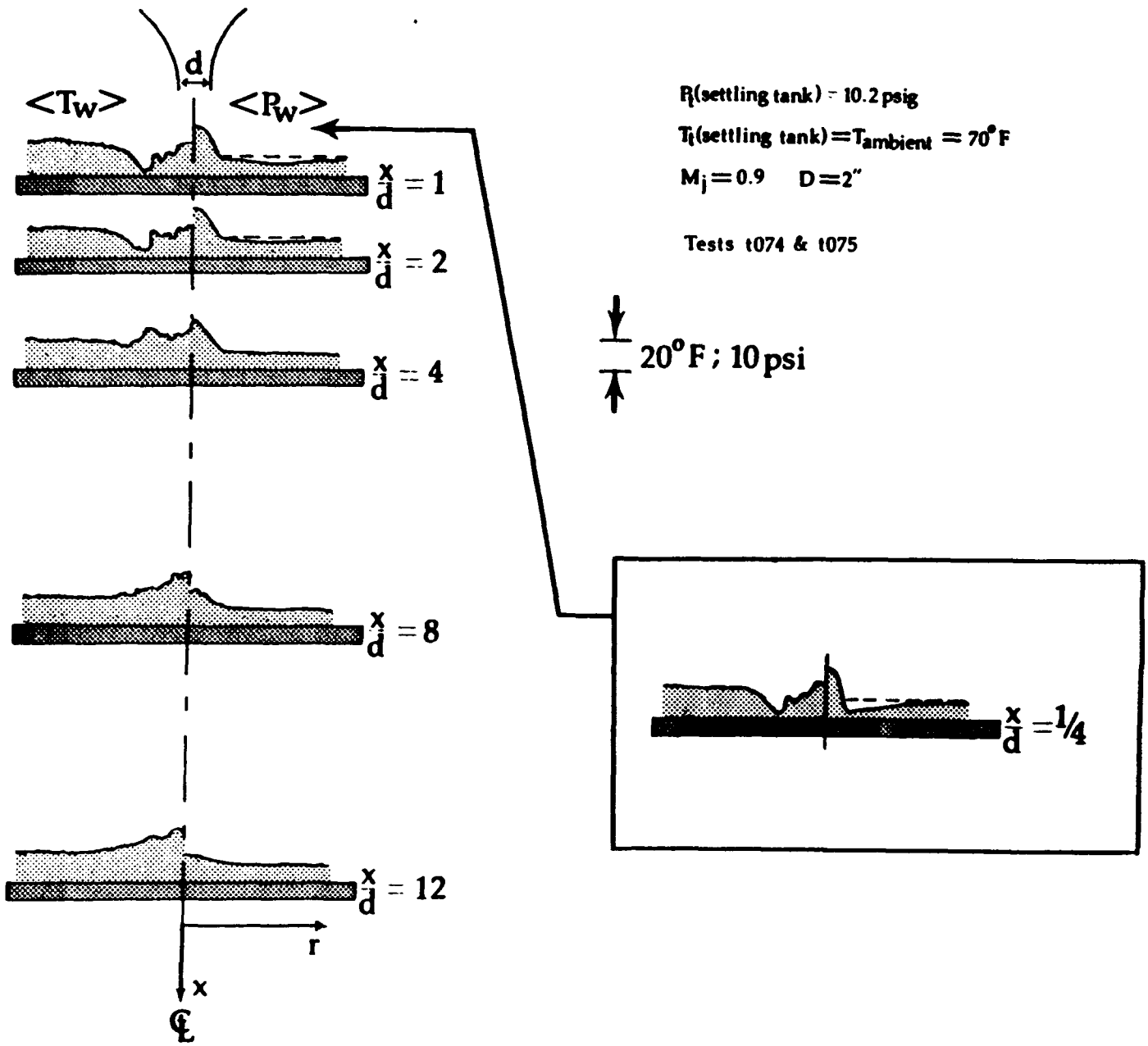

Figure 8. Radial distribution of time-averaged P_w and T_w in an impinging jet.

a "blanket" shielding the impingement plate from the primary vortices. Thus they account for the radial spread of the cooling region. The presence of cooling only in the near field and heating only in the far field is consistent with the presence and absence of the secondary vortices in their respective field.

This T_w data has the same general features as that obtained by Goldstein (Ref. 3) for a low Mach number of 0.1, which were presented without appealing to a vortical structure model of the flow field.

When correlated by x/d and M_j, the T_w data can be divided into two distinct regions: (1) the near field, where $x/d < 2$, and (2) the far field, where $x/d > 4$. As M_j increases, so does the magnitude of T_w separation in each region, as shown in figure 9, which displays the maximum amount of heating and cooling in the radial profile of T_w. In the near-field there is significant cooling and little heating, as mentioned. In the far-field, T_w increases to a maximum value around $x/d = 9$ and then drops as the jet momentum diffuses.

A third region, characterized by spiky peaks of ΔT_c and ΔT_h at $M_j = 0.9$, can be identified between $x/d \sim 2$ and $x/d \sim 4$. In this "transition" region, particularly at high M_j, both heating and cooling are present in the radial profile of T_w. At these seemingly anomalous, uncorrelated points, a loud sound is heard, which will be discussed next.

8.2(b) *Acoustic Interaction*

The sound spectrum as received by the microphone is transformed by the FFT method, and the frequency and magnitude of the dominant peaks are recorded. Figures 10 and 11 plot these dominant frequencies vs. x for 2" and 4" nozzles at $M_j = 0.8$ and $M_j = 0.9$ respectively. Solid lines A and B correspond to equations (2) and (3) of the model. As expected from the theoretical considerations, most acoustic peaks occur when both the convective and standing wave modes fall along the same line. It was discovered that when the standing acoustic wave frequencies and the shedding frequency are close to the resonant frequency of the flow-straightener section, f_v adjusts itself to match this frequency. This "triple resonance" results in a high-magnitude acoustic peak. It is this phenomenon that explains the seemingly uncorrelated T_w values in figure 11 between $x/d \sim 2$ and $x/d \sim 4$.

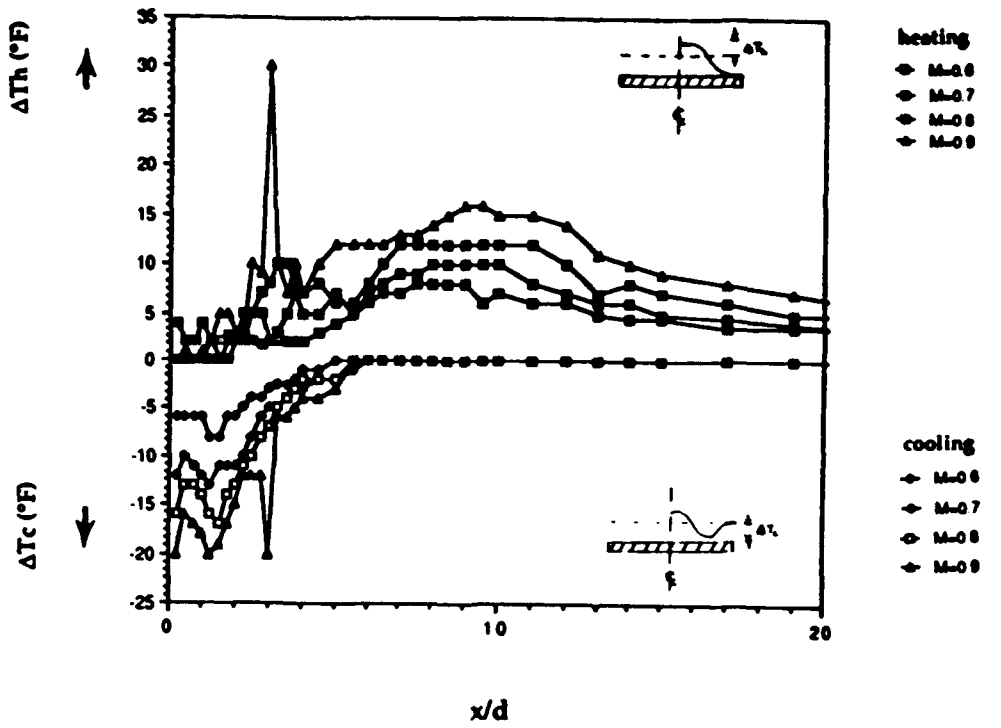

Figure 9. Time-averaged T_w in an impinging jet--correlation of ΔT_h and ΔT_c in terms of x/d and M_j.

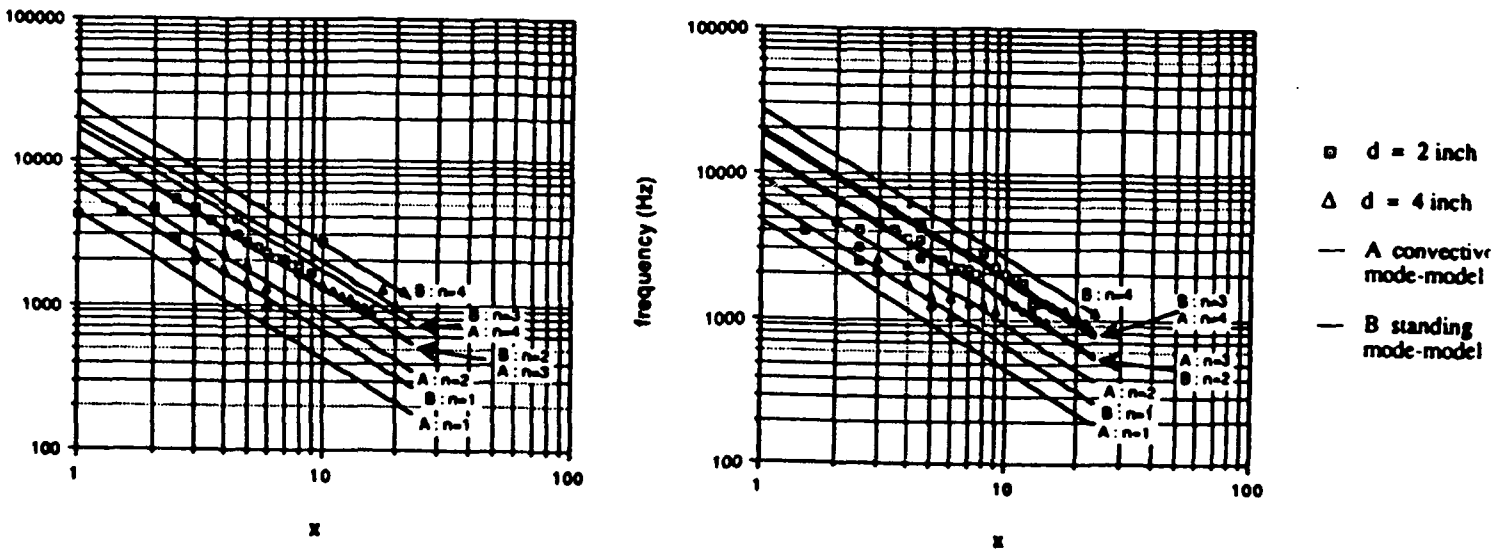

Figure 10 and 11. Correlation of experimental acoustic data with the model for M_j = 0.8 and M_j = 0.9.

To confirm directly the relationship between the uncorrelated points and strong acoustic resonance, sound absorbing foam was placed over the nozzle and data was taken over the entire range of x/d . M_j was held at 0.9, where the effects of resonance were strongest. Figure 12 compares the T_w profiles and their accompanying frequency spectra for the bare nozzle and the acoustically treated nozzle at x/d = 3 (corresponding to the uncorrelated T_w values). This figure shows that suppressing the acoustic resonance eliminated the aforementioned anomalous behavior in the transition region. No change in the results for $x/d < 2$ or $x/d > 4$ was observed, verifying that acoustic resonance is the key to the behavior of T_w in this region.

8.2(c) *'Synthetic' Secondary Vortices*

We wished to confirm that the secondary vortices are indeed responsible for cooling. The primary vortices, which generate secondary vortices on the impingement plate, create their own T_t separation discussed in (7e); this in turn competes and interferes with the T_t separation induced by the secondary vortices. Thus the presence of the primary vortices complicates the issue. If one can create the 'synthetic' secondary vortices, not caused by the primary vortices but by the device which by itself does not induce T_t separation, then one can conclude that cooling is in fact caused by the secondary vortices. A row of vortices created at the interface of free shear flows, for instance, can serve as such 'synthetic' secondary vortices. Although the former are two-dimensional and linear vortices, the latter circular, such a difference in geometry is insignificant in so far as their role in cooling is concerned.

For this, the air facility was modified into a blow-down wind tunnel, fitted with the test section of square cross-section of 3.5" x 3.5". As shown in figure 13, a mesh screen was installed within the test section in order to create the free shear. The result of T_t survey carried out at various downstream locations (Fig. 14) clearly indicates the presence of cooling on the expected side of the vortex (as well as the expected heating on the other side). This appears to lend support to the presence of cooling induced by the secondary vortices.

8.2(d) *Effect of Impingement Surface Curvature*

The curvature of the impingement surfaces causes the pressure gradient along the surface to be different from that of a flat surface. The surface pressure gradient is,

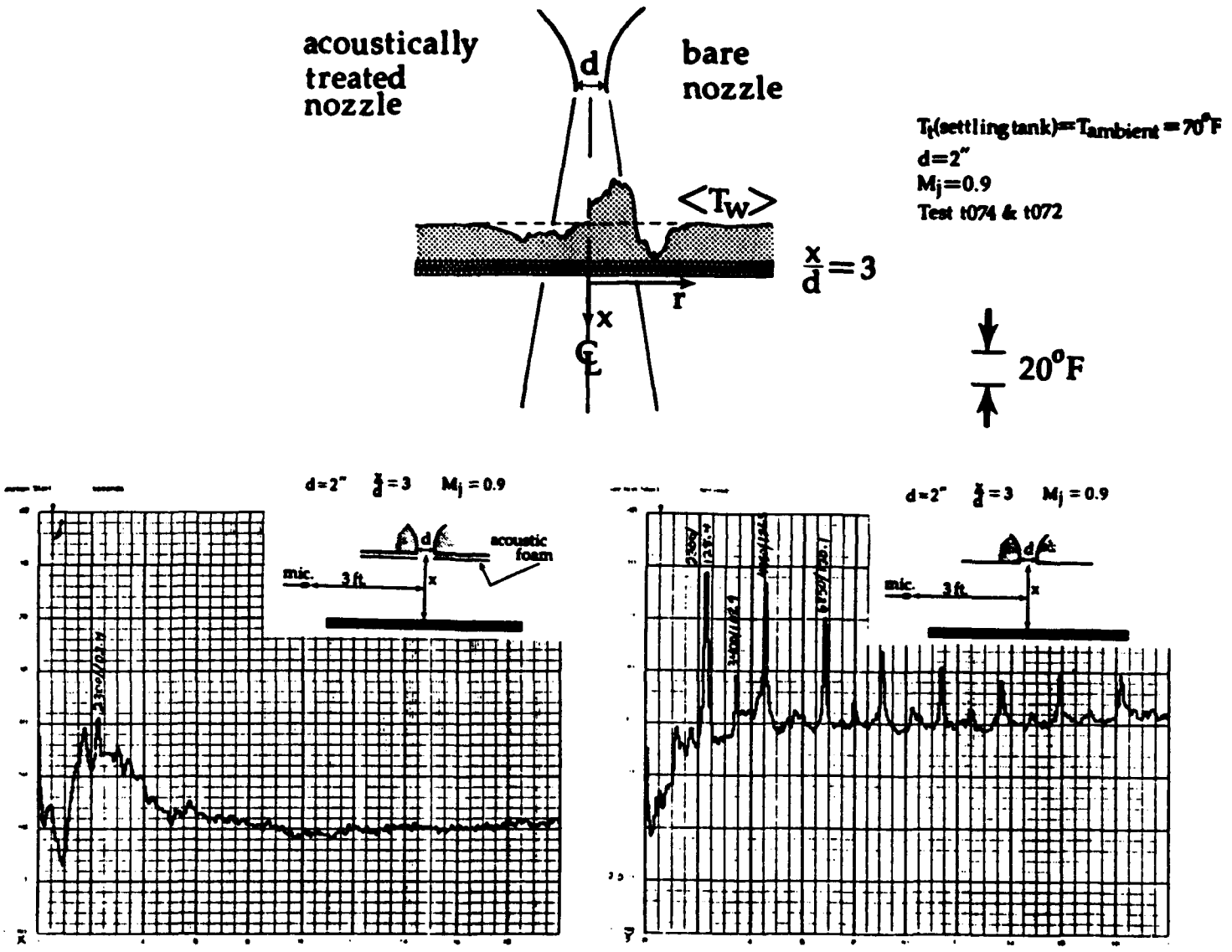

Figure 12. Time-averaged T_w and frequency spectra at acoustic resonance-comparison between bare and acoustically treated nozzle.

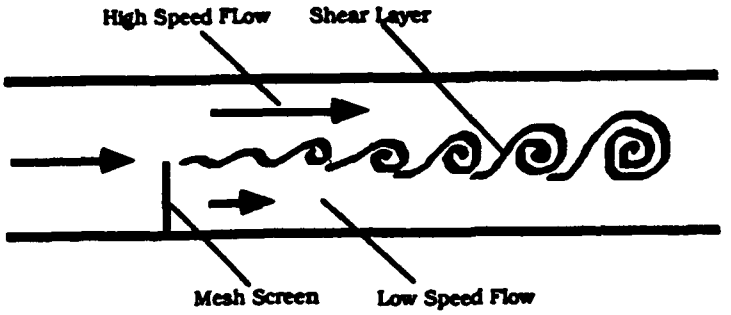

Figure 13. 'Synthetic' secondary vortices in shear flow.

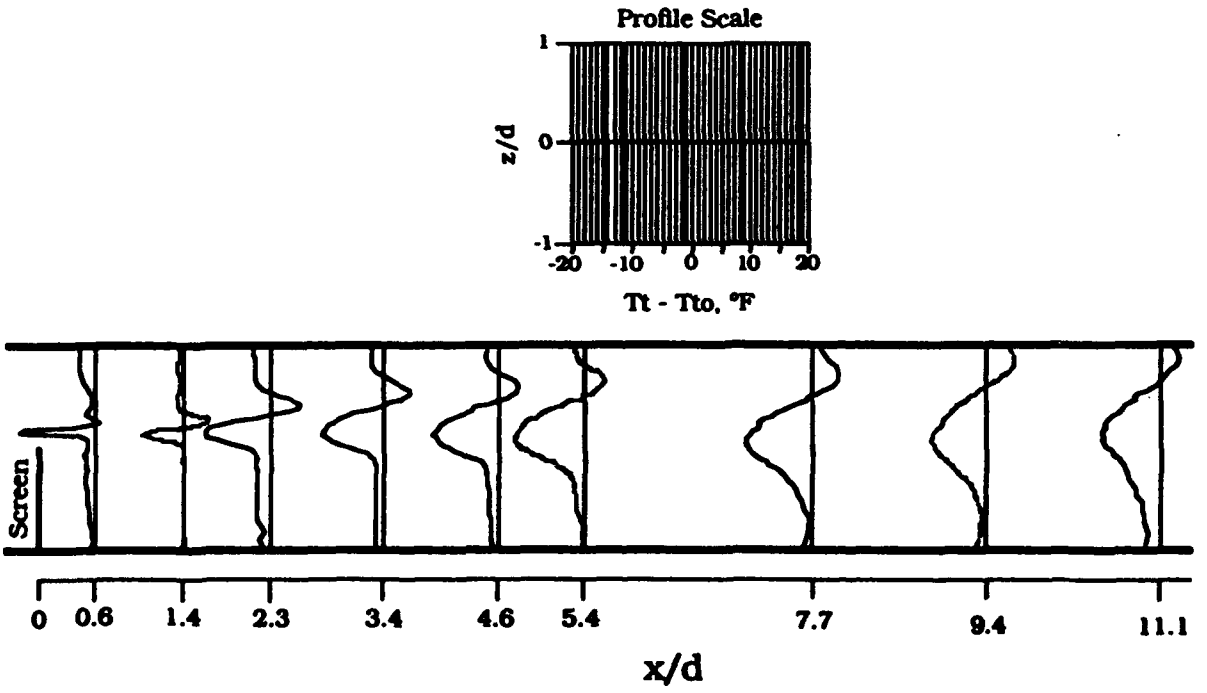

Figure 14. Total temperature profiles behind screen (P_{to} = 10 psig, T_{to} = 69°F).

of course, a steady one. The experimental results for a concave and convex surface (figure 15) shows that the difference in the steady pressure gradient causes insignificant changes in the T_t separation over the surface. This indicates, as expected, that it is primarily the *unsteady* (rather than the steady) pressure field created by the primary vortices that determines the strength of the secondary vortices and the surface T_t distribution.

8.2(e) *Effect of Higher Jet Mach Number*

As already seen in figure 9 for subsonic jets, the amount of wall cooling increases as the jet Mach number increases. Figure 16 shows the corresponding results for higher Mach numbers. Of special interest is the cooling of 74° observed for a sonic jet; this cooling occurs at the jet centerline.

The mechanism of this centerline cooling is not clear at present, although it is speculated that expansion waves generated by the formation of the primary vortices may somehow be responsible for this. Thus 74°F can be scaled, in the turbine environment of 2400°F, to 430°F of cooling.

(9) *Technical publications and presentations*

"Total Temperature in an Impinging Jet" by M.D. Fox, K. Hirano and M. Kurosaka, paper No. CE-5, presented at the 42nd Annual Meeting of the Division of Fluid Dynamics, The American Physical Society, November 19, 1989: *Bulletin of the American Physical Society*, Vol. 34, No. 10, 1989, pp. 2273.

"Total Temperature Separation in an Impinging Jet" by M.D. Fox, M. Kurosaka and K. Hirano, AIAA Paper No. 90-1622, presented at the AIAA 21st Fluid Dynamics, Plasmadynamics and Lasers Conference, June 18-20, Seattle, WA.

"Vortex-Induced Cooling in a Supersonic Impinging Jet" by M.D. Fox and M. Kurosaka, Paper No. HC-7, presented at the 43rd Annual Meeting of the Division of Fluid Dynamics, The American Physical Society, November, 20, 1990; Bulletin of the American Physical Society, Vol. 35, No. 10, 1990, pp. 2307.

"Vortex-Induced Total Temperature Separation in an Obstructed Flow" by J.J. O'Callaghan and M. Kurosaka, Paper No. AB-2, presented at the 43rd Annual Meeting

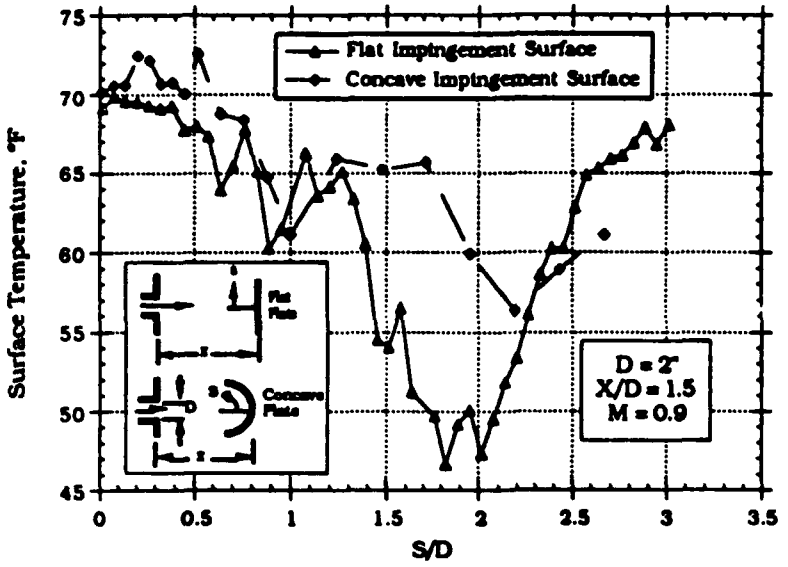

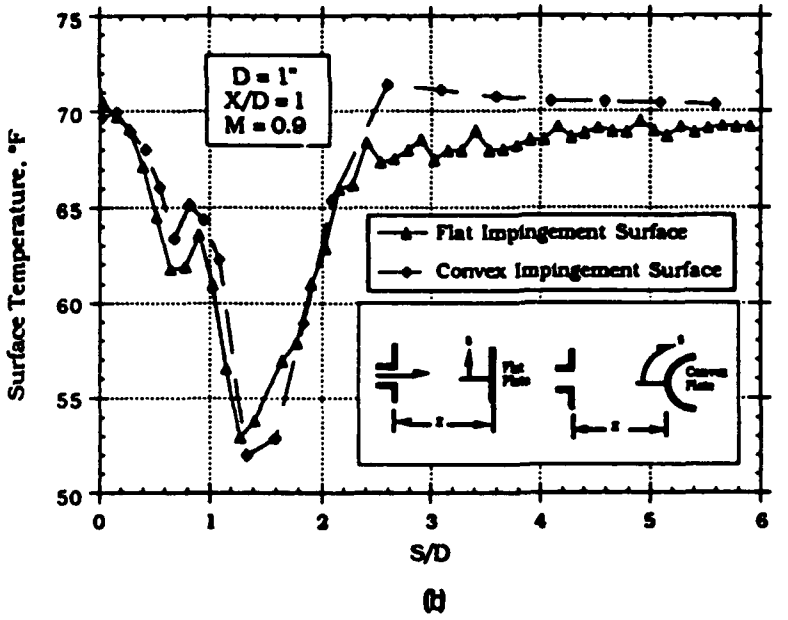

Figure 15.

Temperature measurements on the surfaces of flat, (a) concave, and (b) convex impingement plates.

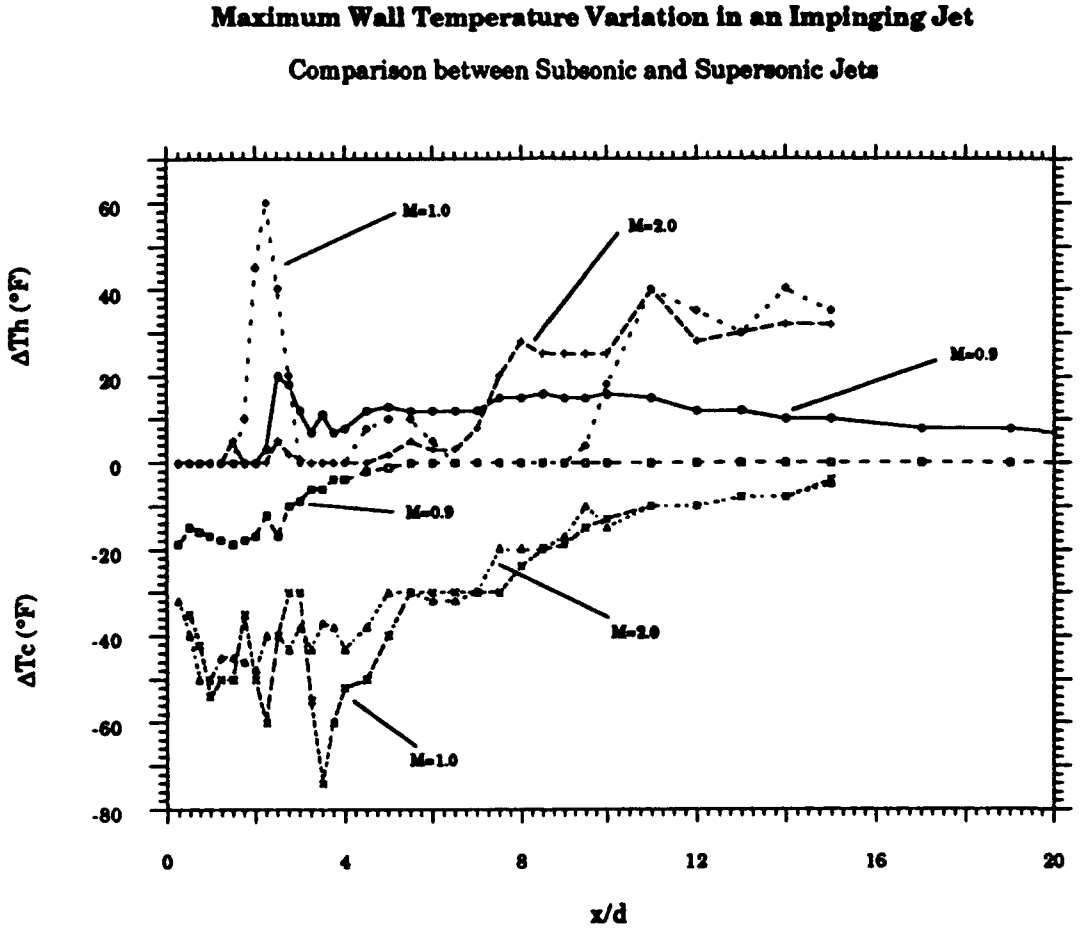

Figure 16. Cooling and heating in sonic and supersonic jets.

of the Division of Fluid Dynamics, The American Physical Society, November 18, 1990; Bulletin of the American Physical Society, Vol.. 35, No. 10, 1990, pp. 2227.

"Vortex-Induced Cooling in Impinging Jets" by M.D. Fox, M. Kurosaka and H. Hirano, to be presented 1991 Yokohama International Gas Turbine Congress, Yokohama, Japan, October, 1991.

"The Energy Separation in Free and Impinging Jets" by M.D. Fox, M. Kurosaka and K. Hirano, to be submitted to the Journal of Fluid Mechanics.

(10) ***Students***

T. L. Li	MS 1989
M. D. Fox	MS 1990, Ph.D. 1993 (expected)
J. J. O'Callaghan	MS 1991

(11) ***Awards***

M. D. Fox - 1990 AIAA Pacific Northwest Student Achievement Award
M. D. Fox - 1990 AIAA Region VI Student Paper Conf., 2nd place in graduate division

References

1. "Energy Separation in a Vortex Street", Kurosaka, M., Gertz, J.B., Graham, J.E., Goodman, J.R., Sundaram, P., Riner, W.D., Kuroda, H. and Hankey, W.L., *Journal of Fluid Mechanics*, Vol. 178, pp. 1-29, 1987.

2. "Time-Resolved Measurements of Total Temperature and Pressure in the Vortex Street Behind a Cylinder", Ng, W.F., Chakroun, W.M. and Kurosaka, M., *Physics of Fluids*, Vol. 2, No. 6, pp. 971-978, 1990.

3. "Streamwise Distribution of the Recovery Factor and the Local Heat Transfer Coefficient to an Impinging Circular Air Jet", Goldstein, R.J., Behbahani, A.I. and Heppelmann, K.K., *International Journal of Heat and Mass Transfer*, Vol. 29, No. 8, pp. 1227-1235, 1986.